IEEE Access
Multidisciplinary | Rapid Review | Open Access Journal

Received June 28, 2017, accepted July 20, 2017, date of publication July 26, 2017, date of current version August 22, 2017.

Digital Object Identifier 10.1109/ACCESS.2017.2731992

An Improved Latin Hypercube Sampling Method to Enhance Numerical Stability Considering the Correlation of Input Variables

QINGSHAN XU[1], (Member, IEEE), YANG YANG[1], YUJUN LIU[1], AND XUDONG WANG[2]
[1]School of Electrical Engineering, Southeast University, Nanjing 210096, China
[2]Electric Power Research Institute, State Grid Tianjin Electric Power Company, Tianjin 300010, China

Corresponding author: Yang Yang (yangyang9296@163.com)

This work was supported in part by the National Natural Science Foundation of China under Grant 51377021 and in part by the Science and Technology Project of SGCC under Grant SGTJDK00DWJS1600014.

ABSTRACT Latin hypercube sampling (LHS) method has difficulty in dealing with non-positive definite correlation matrices by traditional Cholesky decomposition, whereas it may often happen with the increasing scale of input variables. In order to improve the numerical stability of LHS, an improved LHS with modified alternating projections method (L-Mapm) is proposed in this paper. Compared with other two existing modified algorithms, L-Mapm is considered to possess accuracy, speediness, and controllability at the same time. The accuracy and effectiveness of L-Mapm applied to probabilistic load flow are proven by the comparative tests in the IEEE 33-bus system and PG&E 69-bus system. The simulation results show that L-Mapm has the best performance in modification and expands the application of LHS.

INDEX TERMS Latin hypercube sampling, correlation matrix, non-positive definite matrix, Cholesky decomposition, alternating projections method.

I. INTRODUCTION

In recent years, distributed generation technology based on renewable energy such as solar energy and wind power has been widely used [1], [2]. However the output power of photovoltaic power generation and wind power generation has strong randomness due to the influence of the natural environment factors, and the correlation between multiple power sources also needs to be considered.

Probabilistic load flow (PLF), proposed by Barbara Borkowska in 1974, is considered to be an efficient method to solve the problem of uncertainty in load flow calculation [3]. The algorithm of PLF can be divided into three categories: simulation method [4], [5], analytic method [6], [7] and approximation method [8], [9]. Latin hypercube sampling, one of the simulation methods, is proposed to improve the sampling method and to consider the correlation of input variables [10]–[12]. Through stratified sampling, the sample points are uniformly and completely covered in the distribution range of the variables, which can effectively reduce the variance and the sampling scale. Through controlling the correlation, extracted samples can reflect the relationship between input variables more reliably. Current sampling methods include: interval random sampling (IRS) [13], lattice sampling (LS) [14] and important sampling (IS) [15]. The methods of correlation control include: rank Gram-Schmidt algorithm [16], genetic algorithm [17], simulated annealing algorithm [18] and Cholesky decomposition [14], [19]. Cholesky decomposition, as a commonly used control method, is applied in this paper due to its simple and fast calculation. In general, the correlation coefficient matrix is treated as a positive definite matrix in correlation control [14]. However, the correlation of input variables is more complex and may not be positive definite with the increasing scale of distributed generation, which will produce numerical stability problems. And stability is an important feature of measuring algorithms [20], [21]. As we know, Cholesky decomposition can only be used in the positive definite matrix and the probability of the positive definite matrix will be greatly reduced as the dimension of the matrix increases [22].

The problem also occurs in other important areas such as: finance, risk management and dynamic state estimation (DSE). As a result, some methods have been already proposed to modify the correlation matrix to enhance the numerical stability. ''schol'' is an approach offered in the

unscented Kalman filter toolbox and is applied at DSE [23]. Hypersphere decomposition (Hd) and Spectral decomposition (Sd) are proposed to satisfy the correlation matrix as semi-definite and to ensure the VAR calculation produce a positive number in the BGM interest rate option model or market risk management [24]–[26].

However, ''schol'' cannot guarantee accuracy; Hd is too slow to find the optimal result; Sd is unable to control the correcting effect. In order to solve the problem more effectively, an improved LHS based on alternating projections method (L-Mapm) is presented in this paper. The core conception of L-Mapm is alternating projections method, which is proposed to acquire the closest symmetric positive semi-definite matrix in finance as well as in DSE [27], [28]. After a series of studies carried out on IEEE 33-bus and PG&E 69-bus test systems, L-Mapm is proven to have the best performance in comparison with other two algorithms: LHS based on Hd (L-Hd), LHS based on Sd (L-Sd). The performance of Schol is proven to be unstable and inaccurate and it just obtains an inaccurate Cholesky factor to continue the procedure [28]. As a result, Schol is not used as a comparative method. In order to reflect the influence of the correlation, a line representing the independent input variables is also shown: LHS with independent variables (L-Iv).

This paper is organized as follows: the basic ideas of LHS, is described in Section II first. Then section III introduces the principle of the three modified algorithms: Hd, Sd, and Mapm. The performances of these algorithms are investigated in Section IV through the IEEE 33-bus and PG&E 69-bus test systems, and finally, Section V concludes this paper.

II. LATIN HYPERCUBE SAMPLING

The principle of LHS is ''stratified sampling''. Due to the stratified technique, the sample points are covered in the distribution range of the variables uniformly and completely, and the variance is reduced effectively. LHS consists of two main steps: sampling and permutation.

A. SAMPLING

The cumulative distribution function (CDF) of the input variable $X_1 \cdots X_K$ is ranged from 0 to 1, and the scale of CDF is divided into equal intervals. A value is extracted in each interval, and then the sample value is obtained through the transformation of the inverse function.

Due to the differences in the extraction methods in the interval, a variety of methods have been derived: IRS, LS and IS. The sampling principles of the three sampling methods are as follows:

1) IRS: The n_{th} sample of X_k is:

$$x_{kn} = F_{Z_k}^{-1}((n - rand)/N) \tag{1}$$

2) LS: The n_{th} sample of X_k is:

$$x_{kn} = F_{Z_k}^{-1}(\frac{n - 0.5}{N}) \tag{2}$$

3) IS: The formula is:

$$x_{kn} = F_{Z_k}^{-1}(\int_{y_{k,n}}^{x_{k,n}} Z_k(x)dx + \frac{n-1}{N}) \tag{3}$$

Z_k is the CDF of X_k. F^{-1} is the inverse function transformation. The principle of IS is to select the boundary points near the average value of the probability density function, which reflects the sampling theories of ''stratification'' as well as ''importance''. As the convergence is superior to the effect of IRS and LS, this paper uses IS to draw sample [15].

B. PERMUTATION

Since the correlation of extracted samples cannot reflect the real correlation between input variables, we need to control the correlation.

In this paper, the improved Spearman rank correlation coefficient is used to replace the sample values, which can be used to solve the problem of correlation between input variables of various distributions.

The step of the permutation can be summarized as follows:

1) Input variables $X_1 \cdots X_K$ are sampled to get the sample matrix S.

2) A random sequence matrix A is generated and P_A is the corresponding correlation coefficient matrix of A. If P_A is positive definite, it can be decomposed by the Cholesky decomposition: $P_A = Q_A Q_A^T$ where Q_A is a lower triangular matrix.

3) The specified correlation coefficient matrix is P_{set}. Q_{set} is its lower triangular matrix.

4) $D_A = Q_A^{-1}A$, $D_{set} = Q_{set}D_A$. The original sample matrix S is sorted according to D_{set}, and then a desired sample matrix S_{set} can be obtained.

III. MODIFIED ALGORITHM

Cholesky decomposition is an important step in permutation. However, when the correlation matrix is non-positive definite, the decomposition no longer applies. Assume that P is a symmetric matrix, the diagonal elements are 1, and the non-diagonal elements are random numbers in (-1, 1). As can be seen from Table 1, with the dimension of P is increased, the number of the positive definite matrix is greatly reduced [22]. Although P is not a theoretical correlation coefficient matrix, P is close to the form of the correlation coefficient matrix and can be regarded as a correlation coefficient matrix in the estimation.

In order to improve the stability of LHS and expand the application of it, several modified algorithms are proposed.

A. HYPERSPHERE DECOMPOSITION

This method is first applied in the field of finance and risk control. The matrix can be modified to a semi positive definite matrix by using the hypersphere decomposition method when the abnormal value or the asynchronous data destroys the correlation matrix or the risk manager wishes to change the

TABLE 1. Relationship between dimension and the number of positive-definite matrices.

Dim	Num of P	Num of positive
3	1000	634
4	1000	167
5	1000	28
6	1000	1
7	1000	0

correlation matrix. It exactly coincide to the requirement that the correlation matrix in LHS needs to be positive definite to use the Cholesky decomposition.

Hypersphere decomposition can be understood as an iterative process to alter the pre-existing defined matrix to the target correlation matrix. P is a given non-positive target matrix, $\hat{P}$ is the desired matrix that is closest to P. $\hat{P}$ can be constructed as follows:

$$\hat{P} = QQ^T \tag{4}$$

$$q_{ij} = \begin{cases} \cos\theta_{ij} \cdot \prod_{t=1}^{j-1} \sin\theta_{it} & for\ j = 1 \ldots n-1 \\ \prod_{t=1}^{j-1} \sin\theta_{it} & for\ j = n \end{cases} \tag{5}$$

$\{\theta_{ij}\}$ is an arbitrary set of $n \times (n-1)$ dimensional angles. The main diagonal elements of $\hat{P}$ can be ensured to one due to the trigonometric relationship and the requirement that the radius of the unit hypersphere should be equal to one.

In order to modify $\hat{P}$ to approaching P, a suitable error measure can be defined as follows:

$$\varepsilon_a = \left\| P - \hat{P} \right\| \tag{6}$$

Based on the target equation (6), optimization algorithms can be applied to find the matrix which matches the target matrix best. Admittedly the accuracy of the result is at the expense of the time.

B. SPECTRAL DECOMPOSITION N

Spectral decomposition is an empirical method without iterating and we can always get a correlation matrix modified well. The correction step is:

1) P is a correlation matrix, $\{\lambda_i\}$, $\{L_i\}$ are its corresponding eigenvalues and eigenvectors.

$$\begin{aligned} PL_i &= \lambda_i L_i \\ L_i &= [l_{i1}, l_{i2}, \ldots, l_{in}]^T \end{aligned} \tag{7}$$

2) Λ is the diagonal matrix of eigenvalues and is modified to a positive matrix Λ'.

$$\begin{aligned} \Lambda &= diag(\lambda_i) \\ \Lambda' : \lambda_i' &= \begin{cases} \lambda_i & \lambda_i > 0 \\ \varepsilon_b & \lambda_i \le 0 \end{cases} \end{aligned} \tag{8}$$

3) Based on the eigenvectors $\{L_i\}$, a diagonal scaling matrix D can be acquired as :

$$D : d_i = \left[\sum_{t=1}^{n} l_{it}^2 \lambda_t' \right]^{-1} \tag{9}$$

4) The columns of Q' is arrayed by multiplying the eigenvectors with their corresponding modified eigenvalues. Q is the normalized form of Q'. $\hat{P}$ is the corrected correlation matrix constructed by Q.

$$\begin{aligned} Q' &= L\sqrt{\Lambda'}, \quad Q = \sqrt{D}Q' \\ \hat{P} &= QQ^T \end{aligned} \tag{10}$$

The matrix acquired is just similar to the target one intuitively. However, this method has advantages of simple computation and quick speed.

C. MODIFIED ALTERNATING PROJECTIONS METHOD

Modified alternating projections method modifies the principle of the alternating projections method, which is presented to solve the "nearest correlation matrix" problem occurred in the finance industry. Mapm combines the advantages of HD and SD, which possesses high precision as well as fast speed. We can find a nearest matrix through alternating projections method, and the nearest matrix can be "embellished" to ensure symmetric and positive definite. The alternating projections method can be summarized as (11). The output X is proved to be the desired correlation matrix represented by P when the number of iterations is close to infinity [29], [30].

$$\begin{aligned} X &= P_U(P_S(P_U(\cdots P_S(P)))) \to P \\ P_U(P) &= P - diag(diag(P - I)) \\ P_S(P) &= Z \times diag(\max(v_i, 0)) \times Z^T \\ P &= ZAZ^T, \quad A = diag(v_i) \end{aligned} \tag{11}$$

The detailed procedure of alternating projections method is given:

$$\Delta P = 0 \tag{12}$$

$$Y = P \tag{13}$$

while 1 {

$$[E, v] = eig(M) \tag{14}$$

$$v > \tau_1 \cdot \max(g) \to w \tag{15}$$

$$X = [E]_w \cdot [\underbrace{v_w \cdots v_w}_{n}]^T \times [E]_w^T \tag{16}$$

$$if\,(\|Y - X\| / \|X\| < \tau_2)\, break; \tag{17}$$

$$Y = X - diag(diag(X - I)) \tag{18}$$

}

To guarantee symmetric and positive definite, corresponding steps can be taken:

$$[E, v] = eig(X) \tag{19}$$

$$\delta = \tau_3 \max(v) \tag{20}$$

$$X = E \times diag(v) \times E^T \tag{21}$$
$$X_V = diag(X) \tag{22}$$
$$V = sqrt(\max(X_V, \delta)./diag(X)) \tag{23}$$
$$X = diag(V) \times X \cdot [\underbrace{V \cdots V}_{n}] \tag{24}$$
$$X = (X + X^T)/2 \tag{25}$$

X is the final modified correlation matrix. 'eig', 'max', '·', '×', 'diag', 'sqrt', '·/' are MATLAB functions. E is the eigenvector matrix. v is the column vector of eigenvalues. w is the elements: $v > \tau_1 \cdot \max(v)$. $[E]_w$ is the columns of E that refer to w; '$\|X\|$' is the Frobenius norm, which can be described as (X is the n-order matrix):

$$\|X\| = \sqrt{\sum_{i=1}^{n}\sum_{j=1}^{n}|x_{ij}|^2} \tag{26}$$

IV. CASE STUDIES

In order to compare the effect of these three algorithms applied to LHS, a series of studies are carried out on IEEE 33-bus and PG&E 69-bus test systems with MATLAB 2013b, respectively. Some simulation data is set as: $\varepsilon_a = 10^{-4}$, $\varepsilon_b = 10^{-7}$, $\tau_1 = 10^{-7}$, $\tau_2 = 10^{-4}$, $\tau_3 = 10^{-7}$. The span of some lines is very large, and some are too close to distinguish under normal coordinates. So we use the logarithmic coordinates ($y = \ln x$) instead.

A. MODIFICATION OF MATRIX

P is the original non-positive correlation matrix. $\hat{P}$ is the modified matrix. p_{ij}, $\hat{p}_{ij}$ are the elements of P and $\hat{P}$. In order to compare the correction results of three modified algorithms, different dimensions of matrices are selected (n = 3, 5, 8, 10). The correcting effect is calculated by:

$$e_p = \sqrt{\frac{\sum_{i=1}^{n}\sum_{j=1}^{n}(p_{ij} - \hat{p}_{ij})^2}{n^2}} \tag{27}$$

Three algorithms are compared in Fig.1. The corresponding simulation time is presented in Fig.2.

The correctness of Hd is largely influenced by the optimization algorithms. We use the Genetic Algorithm to find the optimal solution. The correcting effect is not good as the simulation time is not long enough. Even so, the time consumed is the longest, far more than others. For example, under the dimension of 8, the simulation time of Hd is 0.402329s, whereas the time of Sd and Mapm is 0.000115s and 0.000286s.

Sd works well in this test case. However, we cannot control the effect of modification. It is treated as an empirical method as we cannot provide the plausibility of the metric but have always found that the results obtained were similar to the desired results. It is a good choice to take it as a starting point for other algorithm or just a fast approximate method to speed up the calculation. For example, a good starting point of Hd can greatly reduce the iteration time.

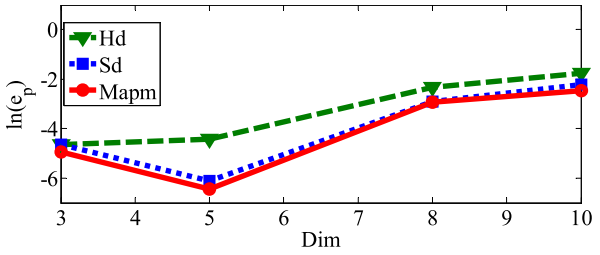

FIGURE 1. Correcting error of three algorithms under different dimensions.

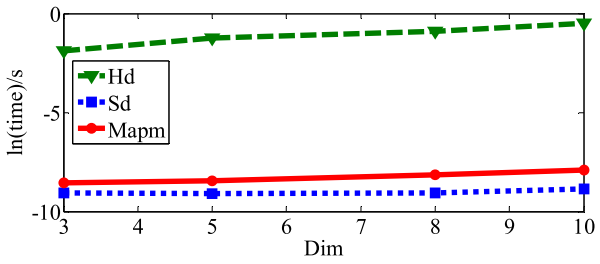

FIGURE 2. Simulation time of three algorithms under different dimensions.

Mapm is considered to have the best effect of correction. The error is minimal and the time is much shorter than Hd. Moreover we can control the precision of the modified matrix through setting the value of τ_2. Mapm is considered to possess accuracy, speediness and controllability at the same time, which ameliorates the problem of the first two algorithms effectively.

B. IEEE 33-BUS

In this study, photovoltaic generation is used as distributed power. The model is based on the Beta distribution, and the shape parameter is set as: $\alpha = 0.9, \beta = 0.85$. The accuracy of the three improved LHS algorithms (L-Hd, L-Sd, L-Mapm) is evaluated by calculating the value of the output variables. Besides, L-Iv is also shown to represent the algorithm of not concerning correlation. The formulas of the relative error are as follows:

$$e^U = \left|\frac{\mu_f^U - \mu_b^U}{\mu_b^U}\right| \times 100\% \tag{28}$$
$$e^P = \left|\frac{\mu_f^P - \mu_b^P}{\mu_b^P}\right| \times 100\% \tag{29}$$
$$\sum e^U == \sum_{i=1}^{N_{node}} e_i^U \tag{30}$$
$$\sum e^P == \sum_{i=1}^{N_{branch}} e_i^p \tag{31}$$

μ_b^U, μ_b^P are the reference value for the voltage and power, which are acquired by large-scale Monte Carlo simulation(MCS). N_{node}, N_{branch} are the total number of nodes and branches of the system. $\sum e^U$, $\sum e^P$ are the sum of relative error of the whole system.

The total number of nodes in the IEEE33 system is: 33; the number of branches: 32; number of links: 5. The distributed photovoltaic generation is connected at the node of 9, 15, 33, and the capacity is: 150kVA. The dimension of correlation matrix is 3.

The MCS was tested under the scale of 40000, 60000 and 80000. The average change rates of voltage and power are 0.0012%, 0.01%; 0.001%, 0.004%. The simulation times are 143.592s, 282.663s, and 437.211s. After comprehensive consideration, the voltage value and power value obtained under the 60000 sampling are selected as the reference value. Four algorithms are tested under the size of 300.

In order to reduce the influence of randomness on the results, four methods are sampled 50 times, and the accuracy and robustness of the algorithm are evaluated by mean value and standard deviation of the 50 relative errors.

Fig.3 and Fig.4 are the mean averages of the relative error of all the voltages and powers. There is no visible correcting problem and all the three modified algorithms work well. However, it should be noticed that the performance of L-Iv is much worse, which confirms that the correlation has great influence on the results of power flow, especially the performance of the voltage. The conclusion can also be validated from the data presented in TAB.II, which is the sum of relative error obtained by the four algorithms. L-Mapm is proved to have the highest precision.

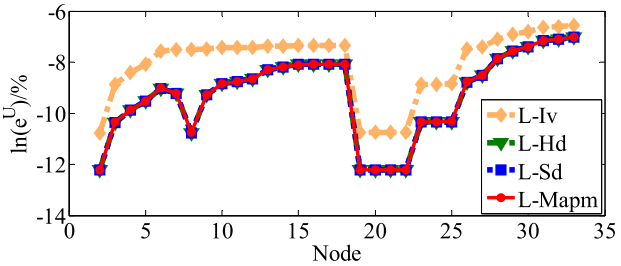

FIGURE 3. The average value of relative error of each node voltage (IEEE-33) obtained by the four algorithms.

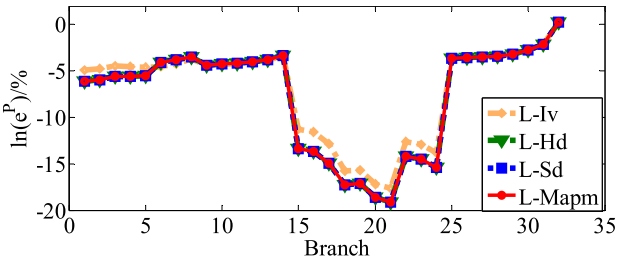

FIGURE 4. The average value of relative error of each branch power (IEEE-33) obtained by the four algorithms.

The standard deviations of the relative error of the three modified algorithms are shown in Fig.5 and Fig.6. L-Mapm is considered to have a better stability as its standard deviations are lower than L-Hd and L-Sd.

TABLE 2. The sum of relative error (IEEE-33) obtained by the four algorithms under the sample size of 300.

N=300	$\sum e^U$ /%	$\sum e^P$ /%
L-Iv	0.00949	0.8722
L-Hd	0.00519	0.8602
L-Sd	0.00514	0.8597
L-Mapm	0.00511	0.8593

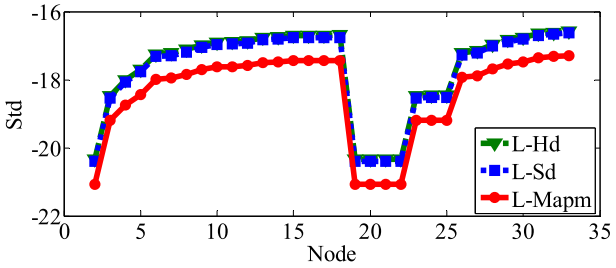

FIGURE 5. standard deviation of relative error of each node voltage (IEEE-33) obtained by the three algorithms.

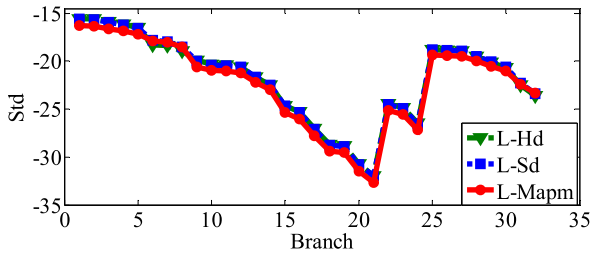

FIGURE 6. The standard deviation of relative error of each branch power (IEEE-33) obtained by the three algorithms.

Next is a detailed analysis of the results of a single sampling. The node voltage and branch power under all sampling values obtained by the four algorithms are shown in Fig.7-8. Local enlarged drawing is adopted to show the distribution of curves more clearly. L-Mapm is considered to have a relatively small fluctuation range, comparing with other algorithms. The probability density functions of node (20) voltage and branch (20) power are shown in Fig.9 and Fig.10. As can be seen, the distributions of L-Hd, L-Sd and L-Mapm are basically consistent with the true distribution, which is represented by MCS, whereas the distribution of L-Iv is rather different from the others.

C. PG&E 69-BUS

The total number of nodes in the PG&E69 node system is: 69; the number of branches: 68; number of links: 5. A big difference of the system distinguished from IEEE33 is that we increases the number of input variables greatly as well as the capacity. The photovoltaic generation is connected at 12, 18, 25, 28, 39, 43, 53, 68, and the capacity is: 200kVA. The dimension of correlation matrix is 8. The purpose of

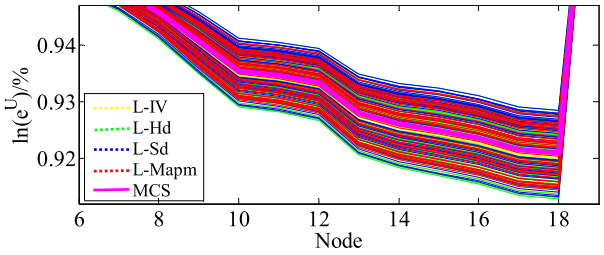

FIGURE 7. The node voltage under all sampling values obtained by the four algorithms and MCS.

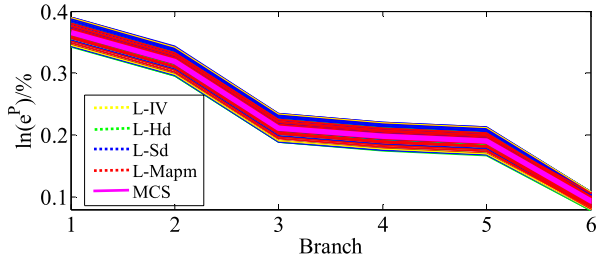

FIGURE 8. The branch power under all sampling values obtained by the four algorithms and MCS.

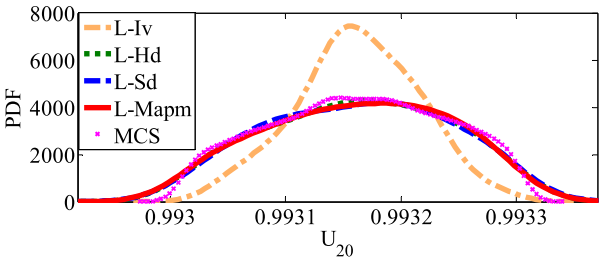

FIGURE 9. The probability density functions of node(20) voltage obtained by the four algorithms and MCS.

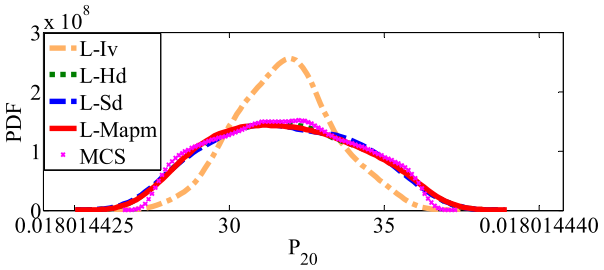

FIGURE 10. The probability density functions of branch(20) power obtained by the four algorithms and MCS.

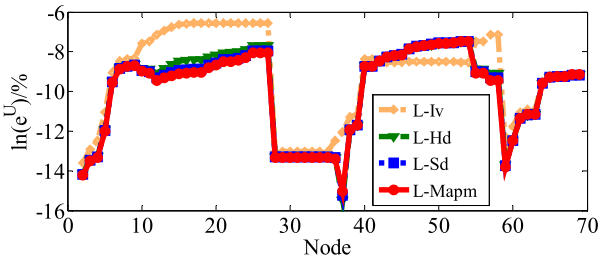

FIGURE 11. The average value of relative error of each node voltage (PG&E-69) obtained by the four algorithms.

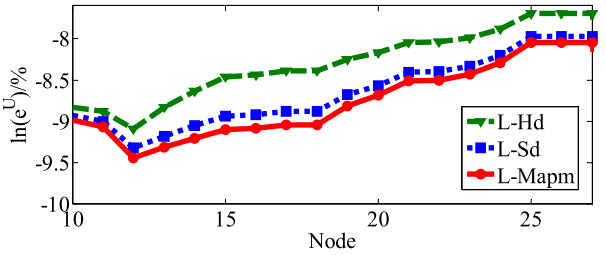

FIGURE 12. Partial enlarged detail of Fig.11.

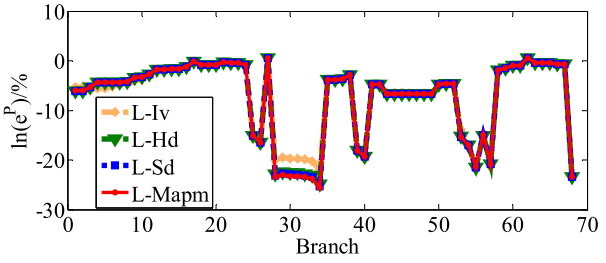

FIGURE 13. The average value of relative error of each branch power (PG&E-69) obtained by the four algorithms.

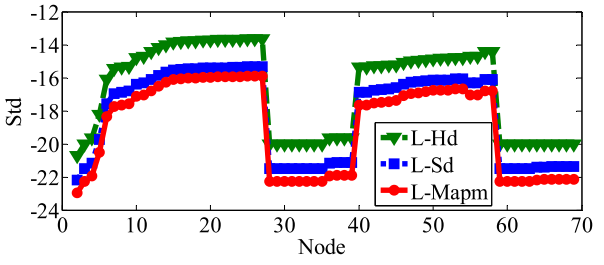

FIGURE 14. The standard deviation of relative error of each node voltage (PG&E-69)obtained by the three algorithms.

this test system is to determine whether these three modified algorithms are stable when the dimension of matrix is larger.

The MCS was tested under the scale of 30000, 50000 and 70000. The average change rates of voltage and power are 0.009%, 0.013%; 0.002%, 0.008%. The simulation times are 193.631s, 456.513s, and 857.044s. The sample of 50000 is chosen as the reference value. Under the scale of 300, all the average values and standard deviations of the relative error tested by four algorithms are shown in Figs.11–15 and Table 3 after repeating 50 times. As we can see, ignoring correlations can lead to significant errors in voltage and power especially in the voltage as the error is twice as much as the others. L-Hd, L-Sd, and L-Mapm seem to have approximate correction effect as before. However, from Fig.12, a partial enlarged detail of Fig.11, we can find that L-Mapm has the most accurate result. This finding is consistent with the result of Fig.1. Moreover L-Mapm still has much better stability than L-Hd and L-Sd.

From a detailed analysis of a single sampling (Fig.16-19), the distribution of L-Mapm is most fitted to the true

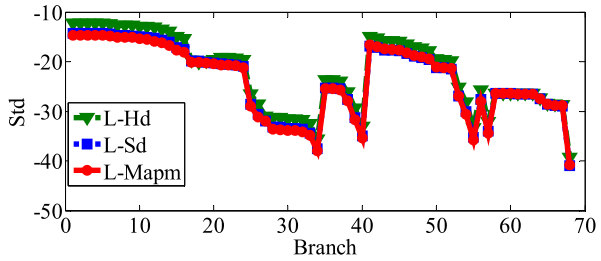

FIGURE 15. The standard deviation of relative error of each branch power (PG&E-69) obtained by the three algorithms.

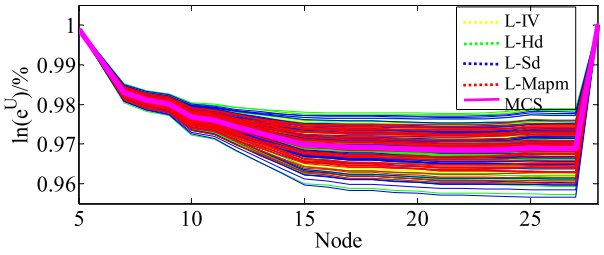

FIGURE 16. The node voltage under all sampling values obtained by the four algorithms and MCS.

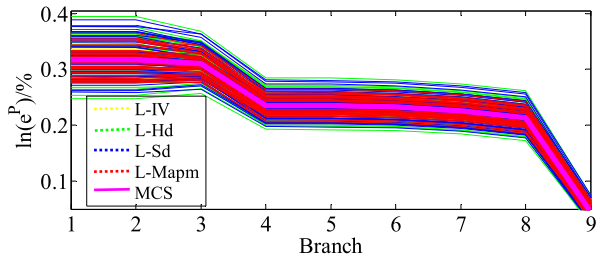

FIGURE 17. The branch power under all sampling values obtained by the four algorithms and MCS.

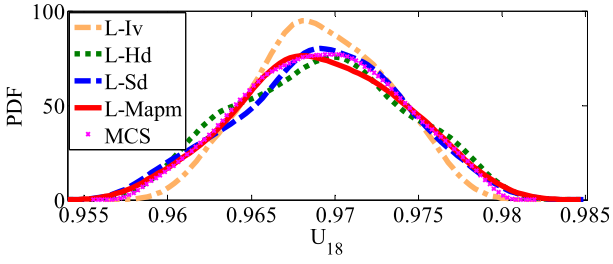

FIGURE 18. The probability density functions of node(18) voltage obtained by the four algorithms and MCS.

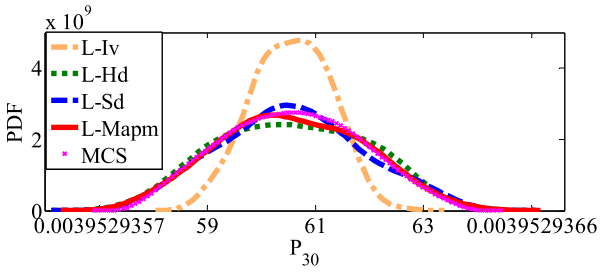

FIGURE 19. The probability density functions of branch(31) power obtained by the four algorithms and MCS.

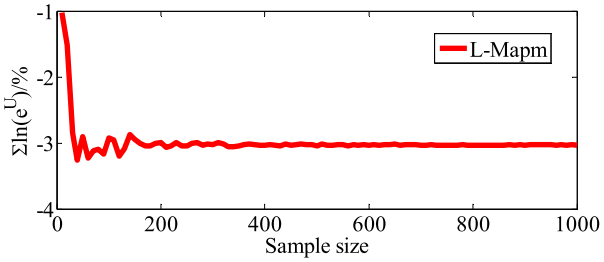

FIGURE 20. The sum of the relative error of node voltage under different sample size.

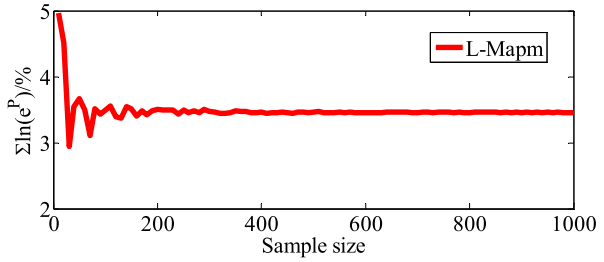

FIGURE 21. The sum of the relative error of branch power under different sample size.

TABLE 3. The sum of relative error (PG&E-69) obtained by the four algorithms under the sample size of 300.

N=300	$\sum e^U$ /%	$\sum e^P$ /%
L-Iv	0.03954	8.6552
L-Hd	0.02346	8.5473
L-Sd	0.02197	8.4509
L-Mapm	0.02008	8.3408

distribution, which is represented by MCS. However, the curve of L-Iv is still far from the reference curve, which cannot reflect the true fluctuations in voltage or power. Moreover, it will directly affect the judgment of bus voltage violation and branch overload.

The sums of the relative error under different sampling sizes are shown in Fig.20 and Fig.21, sampling size from 10 to 1000, with a change of units by 10. Except the beginning of some points, L-Mapm remains a good and steady correcting effect with the increasing of the scale. It also indicates that sufficient samples should be extracted to ensure the accuracy of algorithms.

V. CONCLUSIONS

In this paper, an improved LHS method (L-Mapm) is proposed to enhance the numerical stability of LHS. In order to evaluate the performance of L-Mapm comprehensively, other two modified algorithms (L-Hd, L-Sd) are also introduced. After a series of case studies, the following conclusions can be drawn:

1) Through modifying the matrix under different dimensions, we find that Hd does not own the highest precision but costs the longest time. Sd works well but cannot be controlled. The correcting error of Mapm is the minimal, and Mapm is considered to have the best performance in these three algorithms due to its accuracy, speediness and controllability.

2) In IEEE33 test system: there is no visible correcting problem and all the three algorithms work well. In PG&E69 test system: the difference between algorithms becomes larger, and L-Mapm still has the highest accuracy and best robustness. L-Mapm modifies the problem of numerical stability effectively and expands the application of LHS.

3) The correlation has a great influence on the calculation results of the power flow. Ignoring the correlation cannot reflect the real distribution of the voltage and power, which affects the judgment of the bus voltage violation and branch overload and causes a great error.

4) In PG&E69 test system: L-Mapm is steady except the several fewer sampling points, and sufficient samples should be extracted to ensure the accuracy of algorithms.

REFERENCES

[1] R. A. Jabr, "Adjustable robust OPF with renewable energy sources," *IEEE Trans. Power Syst.*, vol. 28, no. 4, pp. 4742–4751, Nov. 2013.

[2] J. Liu, S. Vazquez, L. Wu, A. Marque, H. Gao, and L. G. Franquelo, "Extended state observer-based sliding-mode control for three-phase power converters," *IEEE Trans. Ind. Electron.*, vol. 64, no. 1, pp. 22–31, Jan. 2017.

[3] B. Borkowska, "Probabilistic load flow," *IEEE Trans. Power App. Syst.*, vol. PAS-93, no. 3, pp. 752–759, May 1974.

[4] B. Zou and Q. Xiao, "Solving probabilistic optimal power flow problem using quasi Monte Carlo method and ninth-order polynomial normal transformation," *IEEE Trans. Power Syst.*, vol. 29, no. 1, pp. 300–306, Jan. 2014.

[5] G. Carpinelli, P. Caramia, and P. Varilone, "Multi-linear Monte Carlo simulation method for probabilistic load flow of distribution systems with wind and photovoltaic generation systems," *Renew. Energy*, vol. 76, pp. 283–295, Apr. 2015.

[6] D. Villanueva, A. E. Feijóo, and J. L. Pazos, "An analytical method to solve the probabilistic load flow considering load demand correlation using the DC load flow," *Electr. Power Syst. Res.*, vol. 110, pp. 1–8, May 2014.

[7] M. J. Chen, Y. Q. Chen, W. C. Dong, and B. Wu, "Containing wind farm power system probabilistic optimal power flow calculation using the method of combined Cumulants and Gram–Charlier expansion," *Adv. Mater. Res.*, vols. 1070–1072, pp. 193–199, Dec. 2015.

[8] M. Mohammadi, A. Shayegani, and H. Adaminejad, "A new approach of point estimate method for probabilistic load flow," *Int. J. Elect. Power Energy Syst.*, vol. 51, no. 10, pp. 54–60, 2013.

[9] C. Delgado and J. A. Domínguez-Navarro, "Point estimate method for probabilistic load flow of an unbalanced power distribution system with correlated wind and solar sources," *Int. J. Elect. Power Energy Syst.*, vol. 61, pp. 267–278, Oct. 2014.

[10] D. Cai, D. Shi, and J. Chen, "Probabilistic load flow computation using Copula and Latin hypercube sampling," *IET Generat., Transmiss. Distrib.*, vol. 8, no. 9, pp. 1539–1549, 2014.

[11] Y. Chen, J. Wen, and S. Cheng, "Probabilistic load flow method based on Nataf transformation and Latin hypercube sampling," *IEEE Trans. Sustain. Energy*, vol. 4, no. 2, pp. 294–301, Apr. 2013.

[12] D. Cai, D. Shi, and J. Chen, "Probabilistic load flow computation with polynomial normal transformation and Latin hypercube sampling," *IET Generat., Transmiss. Distrib.*, vol. 7, no. 5, pp. 474–482, 2013.

[13] B. Minasny and A. B. Mcbratney, "A conditioned Latin hypercube method for sampling in the presence of ancillary information," *Comput. Geosci.*, vol. 32, no. 9, pp. 1378–1388, 2006.

[14] H. Yu, C. Y. Chung, K. P. Wong, H. W. Lee, and J. H. Zhang, "Probabilistic load flow evaluation with hybrid Latin hypercube sampling and Cholesky decomposition," *IEEE Trans. Power Syst.*, vol. 24, no. 2, pp. 661–667, May 2009.

[15] A. Olsson, G. Sandberg, and O. Dahlblom, "On Latin hypercube sampling for structural reliability analysis," *Struct. Safety*, vol. 25, no. 1, pp. 47–68, 2003.

[16] A. B. Owen, "Controlling correlations in Latin hypercube samples," *J. Amer. Statist. Assoc.*, vol. 89, no. 428, pp. 1517–1522, 1994.

[17] M. Liefvendahl and R. Stocki, "A study on algorithms for optimization of Latin hypercubes," *J. Statist. Planning Inference*, vol. 136, no. 9, pp. 3231–3247, 2006.

[18] M. Vorechovský and D. Novák, "Correlation control in small-sample Monte Carlo type simulations I: A simulated annealing approach," *Probab. Eng. Mech.*, vol. 24, no. 3, pp. 452–462, 2009.

[19] M. Hajian, W. D. Rosehart, and H. Zareipour, "Probabilistic power flow by Monte Carlo simulation with Latin supercube sampling," *IEEE Trans. Power Syst.*, vol. 28, no. 2, pp. 1550–1559, May 2013.

[20] J. Liu, W. Luo, X. Yang, and L. Wu, "Robust model-based fault diagnosis for PEM fuel cell air-feed system," *IEEE Trans. Ind. Electron.*, vol. 63, no. 5, pp. 3261–3270, May 2016.

[21] P. R. Kumar, R. S. Kaarthik, K. Gopakumar, J. I. Leon, and L. G. Franquelo, "Seventeen-level inverter formed by cascading flying capacitor and floating capacitor H-bridges," *IEEE Trans. Power Electron.*, vol. 30, no. 7, pp. 3471–3478, Jul. 2015.

[22] X. Xu and Z. Yan, "Probabilistic load flow evaluation considering correlated input random variables," *Int. Trans. Elect. Energy Syst.*, vol. 26, no. 3, pp. 555–572, 2016.

[23] J. Hartikainen, A. Solin, and S. Särkkä, "Optimal filtering with Kalman filters and smoothers—A manual for MATLAB toolbox EKF/UKF," Dept. Biomed. Eng. Comput. Sci., Aalto Univ. School Sci., Greater Helsinki, Finland, Tech. Rep., Aug. 2011.

[24] R. Rebonato, "Calibrating the BGM model," *Risk*, vol. 12, no. 3, pp. 88–94 1999.

[25] R. Rebonato, "On the simultaneous calibration of multi-factor log-normal interest-rate models to Black volatilities and to the correlation matrix," in *Proc. Conf. Global Derivatives*, 1999, vol. 2. no. 2, pp. 277–283.

[26] R. Rebonato and P. Jaeckel, "The most general methodology to create a valid correlation matrix for risk management and option pricing purposes," *Soc. Sci. Electron.*, vol. 32, no. 5, pp. 1–11, 2001.

[27] N. J. Higham, "Computing the nearest correlation matrix—A problem from finance," *IMA J. Numer. Anal.*, vol. 22, no. 3, pp. 329–343, 2002.

[28] J. Qi, K. Sun, J. Wang, and H. Liu, "Dynamic state estimation for multi-machine power system by unscented Kalman filter with enhanced numerical stability," *IEEE Trans. Smart Grid*, to be published.

[29] S.-P. Han, "A successive projection method," *Math. Program.*, vol. 40, nos. 1–3, pp. 1–14, 1988.

[30] J. P. Boyle and R. L. Dykstra, "A method for finding projections onto the intersection of convex sets in Hilbert spaces," in *Advances in Order Restricted Statistical Inference*. New York, NY, USA: Springer, 1986, pp. 28–47.

QINGSHAN XU (M'09) was born in China in 1979. He received the B.S. degree from Southeast University, Nanjing, China, in 2000, the M.S. degree from Hohai University, Nanjing, in 2003, and the D.E. degree from Southeast University in 2006, all in electrical engineering. He was a Visiting Scholar and cooperated with the Aichi Institute of Technology, Toyota, Japan, from 2007 to 2008. He is currently an Associate Professor with Southeast University. His research interests include renewable energy and power system operation and control.

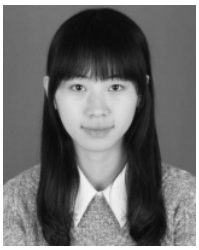

YANG YANG received the B.S. degree in electrical engineering and automation from the Nanjing University of Science and Technology, Nanjing, China, in 2016. She is currently pursuing the M.S. degree in electrical engineering with Southeast University, Nanjing. Her research interests include probabilistic load flow and renewable energy.

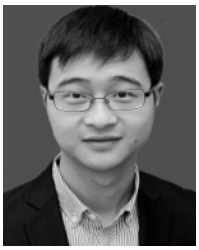

YUJUN LIU received the B.Sc. degree in electrical engineering from Sichuan University, Chengdu, China, in 2010, and the Ph.D. degree in electrical engineering from Southeast University, Nanjing, China, in 2015. He is currently a Post-Doctoral Research Associate with Southeast University. His research interests include vehicle-to-grid technology, active distribution system, energy storage system, and load estimation.

XUDONG WANG is a Senior Engineer. His research direction is power grid operation analysis and control, distribution system automation.